Insights into the molecular basis of the differing susceptibility of varying cell types to the toxicity of amyloid aggregates

Cristina Cecchi[1,4], Serena Baglioni[1], Claudia Fiorillo[1], Anna Pensalfini[1], Gianfranco Liguri[1,4], Daniele Nosi[2], Stefania Rigacci[1], Monica Bucciantini[1,4] and Massimo Stefani[1,3,4,*]

[1]Department of Biochemical Sciences, [2]Department of Anatomy, Histology and Forensic Medicine, [3]Center of Excellence for Molecular and Clinical Studies in Chronic, Inflammatory, Degenerative and Tumoural Diseases for the Development of New Therapies and [4]Interuniversity Centre for the Study of the Molecular Basis of Neurodegenerative Diseases, University of Florence, Florence, 50134, Italy

*Author for correspondence (e-mail: stefani@scibio.unifi.it)

Accepted 19 April 2005
Journal of Cell Science 118, 3459-3470 Published by The Company of Biologists 2005
doi:10.1242/jcs.02473

Summary

It has been reported that different tissue or cultured cell types are variously affected by the exposure to toxic protein aggregates, however a substantial lack of information exists about the biochemical basis of cell resistance or susceptibility to the aggregates. We investigated the extent of the cytotoxic effects elicited by supplementing the media of a panel of cultured cell lines with aggregates of HypF-N, a prokaryotic domain not associated with any amyloid disease. The cell types exposed to early, pre-fibrillar aggregates (not mature fibrils) displayed variable susceptibility to damage and to apoptotic death with a significant inverse relation to membrane content in cholesterol. Susceptibility to damage by the aggregates was also found to be significantly related to the ability of cells to counteract early modifications of the intracellular free Ca^{2+} and redox status. Accordingly, cell resistance appeared related to the efficiency of the biochemical equipment leading any cell line to sustain the activity of Ca^{2+} pumps while maintaining under control the oxidative stress associated with the increased metabolic rate. Our data depict membrane destabilization and the subsequent early derangement of ion balance and intracellular redox status as key events in targeting exposed cells to apoptotic death.

Key words: Amyloid toxicity; Pre-fibrillar protein aggregates; Conformational diseases; Folding and disease; Protein misfolding and citotoxicity.

Introduction

The data reported in the past few years have considerably improved the knowledge of the molecular basis of protein misfolding and aggregation, as well as of the relationship between structure and toxicity of the amyloid aggregates (Dobson, 2003). Indeed, the idea that the most highly toxic species are the pre-fibrillar aggregates whereas mature fibrils are substantially harmless is currently gaining increasing support (Walsh et al., 2002; Stefani and Dobson, 2003; Kayed et al., 2003). These data have led to the proposition that the pre-fibrillar assemblies share basic structural features that, at least in most cases, seem to underlie common biochemical mechanisms of cytotoxicity (Stefani and Dobson, 2003; Kayed et al., 2003; Bucciantini et al., 2002; Bucciantini et al., 2004, Bucciantini et al., 2005).

A number of biochemical modifications eventually leading to cell death have been reported in cells exposed to toxic aggregates of several differing peptides and proteins either in whole animals or in differing cultured cell lines (Lane et al., 1998; Morishima et al., 2001; Velez-Pardo et al., 2001; Zhang et al., 2002; Ross, 2002; Bhagat et al., 2002; Iijima et al., 2004; Bucciantini et al., 2004). These comprise an imbalance of the intracellular redox status and free Ca^{2+} levels (reviewed in Stefani and Dobson, 2003) together with a number of other characteristics, such as derangement of lipid homeostasis (Janciauskiene and Ahrén, 2000), interaction with membrane receptors (Mruthinti et al., 2003) and, in the case of aggregates of proteins containing poly(Q) extensions, dysregulation of the transcriptional machinery (Sakahira et al., 2002). One leading hypothesis of the molecular basis of amyloid toxicity claims that single misfolded molecules or a subpopulation of pre-fibrillar aggregates interacts with the cell membrane disassembling the lipid bilayer (Yip and McLaurin, 2001; Green et al., 2004); the resulting impairment of membrane permeability would then lead to an imbalance of ion homeostasis (Kourie and Henry, 2002). Indeed, modifications of ion permeability have been found in cells exposed to amyloid aggregates; in particular, alterations of the intracellular free Ca^{2+} levels have been repeatedly reported (reviewed in Dobson, 2003). The latter is considered a key modification determining the fate of a cell in terms of life or death; indeed, a rise of free Ca^{2+} may trigger apoptosis indirectly, by affecting mitochondrial functionality and/or directly, by activating caspases and calpains (Orrenius et al., 2003).

Usually, in cells, the rise of free Ca^{2+} is associated with the elevation of ROS, possibly following the activation of the oxidative metabolism to couple the increased need for ATP by the calcium pumps (Squier, 2001). In turn, ROS increase may reinforce the rise of free Ca^{2+} by inhibiting the Ca^{2+} pumps

(Squier, 2001; Orrenius et al., 2003). Despite this and other information, the biochemical modifications in cells exposed to the toxic aggregates are far from being well known.

The role of membrane lipid composition in favouring or disfavouring protein peptide aggregation at the cell surface, and the following membrane structural and biochemical alterations have also not yet been investigated in detail. There is evidence that protein conversion into toxic aggregates is enhanced by membranes (Lee et al., 2003; Bokvist et al., 2004) and by increased levels of anionic phospholipids, such as phosphatidylserine (PS), in neuronal membranes of Alzheimer's disease patients (Wells et al., 1995). Increased PS content is also found at the outer surface of the plasma membrane of neuronal cells, thus providing a possible explanation of the higher susceptibility of the latter to the toxic insult of folding variants of proteins (Svanborg at al., 2003). The role of membrane cholesterol in neurodegenerative diseases is highly controversial (Ledesma and Dotti, 2005), and there are reports indicating that loss of neuronal membrane cholesterol may be detrimental by favouring amyloid peptide generation (Abad-Rodriguez et al., 2004).

In general, it is believed that surfaces can catalyze the formation of amyloid fibrils with mechanisms substantially different from those occurring in bulk solution (Zhu et al., 2002) and that self-assembly on the bilayer surface is critical for membrane disruption (Yip and McLaurin, 2001). The interaction with suitable surfaces can favour protein aggregation by surface concentration resulting from the two-dimensional nature of the association; the interaction may also induce conformational changes leading to aggregation-prone conformers (Bokvist et al., 2004). However, much of this knowledge has been achieved mainly with synthetic membranes, whereas we still lack a deeper knowledge of the relationship between lipid composition of cell membranes, cell susceptibility to the toxic aggregates and mechanisms of aggregate cytotoxicity.

Another, possibly related yet poorly investigated, issue is the biochemical/molecular basis of the differing susceptibility to the toxic insult by the aggregates of different cell types either in whole organisms (Soriano et al., 2003) or in culture (Mazziotti and Perlmutter, 1998; Dargusch and Schubert, 2002). For example, the basal forebrain cholinergic neurons in one of the vulnerable areas in Alzheimer's disease brain are reported to be most consistently and severely affected by Abeta peptides (Hohmann et al., 1988) although the cause of this preferential decimation remains unknown. Several reports show that differing cultured cell lines are variously affected by aggregates of Abeta peptides and amylin, even in relation to differentiation (Janciauskiene and Ahrén, 1998; Janciauskiene and Ahrén, 2000; Sung et al., 2003). The biochemical features of the reduced sensitivity to amyloid aggregate toxicity displayed by resistant elements selected among populations of cultured PC12 cells have been studied (Mazziotti and Perlmutter, 1998; Sung et al., 2003). It has also been reported that in primary cultures of mouse brain cells neurons are most heavily affected by toxic Abeta 42 aggregates than glia cells (Bloom et al., 2005) and that the latter are the primary target of Abeta aggregates whose effects subsequently affect neuronal viability (Abramov et al., 2004). Finally, it has been claimed that one of the most perplexing aspects of polyglutamine disorders is the degeneration of particular neuronal populations in the presence of poly(Q) aggregates, although the aggregating poly(Q) protein is much more widely expressed across the brain (reviewed in Michalik and Van Broeckhoven, 2003).

In all these cases, the enhanced resistance of cells has been attributed to adaptive mechanisms reducing the sensitivity to oxidative stress. However, the latter does not seem, by itself, sufficient to complete the death program in sensitive cells (Soriano et al., 2003) and the increased anti-oxidant defences do not seem to account entirely for the survival of resistant cells (Mazziotti and Perlmutter, 1998).

A deeper knowledge of the biochemical modifications underlying the increased resistance of cells to death following exposure to toxic aggregates appears mandatory to improve our understanding of the chain of events eventually causing exposed cells to die. To address this question, we have performed a study on a panel of cultured normal or pathological cell lines. The culture media of these cells were supplemented with the same amount of pre-fibrillar or fibrillar aggregates of a protein unrelated to any protein deposition disease, the N-terminal domain of the prokaryotic hydrogenase maturation factor HypF (HypF-N)*, previously shown to impair (in the form of pre-fibrillar aggregates) the viability of exposed NIH-3T3 and PC12 cells (Bucciantini et al., 2002). More recently, we have found that NIH-3T3 cells exposed to these aggregates undergo early intracellular free Ca^{2+} and ROS increases eventually leading to cell death (Bucciantini et al., 2004) similarly to cells exposed to aggregates of a number of peptides and proteins associated with amyloid diseases (Sousa et al., 2001; Caughey and Lansbury, 2003). We found that the investigated cell lines displayed very different susceptibility or resistance to the toxic aggregates of our model protein. Also, we show that the different impairment of cell viability was significantly related to the cholesterol content in the cell membrane and to the differing ability of each cell line to buffer free Ca^{2+} increase and ROS production.

Materials and Methods

Materials

All reagents were of analytical grade or the highest purity available. Cholesterol oxidase, phospholipase C, polyoxyetanyl-cholesteryl sebacate, Congo Red and chemicals, unless otherwise stated, were purchased by Sigma (Milan, Italy). Fura2-acetoxymethyl ester (Fura2-AM), Fluo3-acetoxymethyl ester (Fluo3-AM) and pluronic acid F127 were purchased from Molecular Probes (Eugene, OR). PVDF Immobilio-P Transfer Membrane was obtained from Millipore Corporation (Bedford, MA). The cytosol/mitochondria fractionation kit and C2-10 anti-PARP monoclonal antibody were from Oncogene Research Products (San Diego, CA); rabbit anti caspase-3/CPP32 polyclonal antibodies from Biosource International (CA, USA); anti-Bcl-2 monoclonal antibodies from Santa Cruz Biotech (Santa Cruz, CA). HypF-N was expressed and purified as previously described (Chiti et al., 2001). HypF-N aggregates were obtained by incubating the monomeric protein (0.3 mg ml^{-1}) in 50 mM acetate buffer, pH 5.5 in the presence of 30% (v/v) TFE at room temperature for 48 hours. Under these conditions, homogeneous populations of pre-fibrillar aggregates about 4-8 nm wide and 20-60 nm short were present, as confirmed by transmission electron microscopy (not shown); by prolonging the incubation to 20 days all aggregates appeared as long unbranched fibrils 3-5 or 7-9 nm wide (Bucciantini et al., 2002).

Cell culture and exposure to HypF-N aggregates

Murine C2C12 skeletal myoblasts, rat L6 skeletal myoblasts, human SH-SY5Y neuroblastoma cells, human HeLa adenocarcinoma cells, human IMR90 pulmonary fibroblasts, human A549 carcinoma cells, human A431 epidermoid carcinoma cells and monkey COS7 renal cells were obtained from the A.T.C.C. (Manassas, VA); bovine CPA47 pulmonary artery cells were from the Istituto Zooprofilattico Sperimentale della Lombardia e dell'Emilia, Brescia, Italy; murine Hend endothelium cells were a kind gift of Professor F. Bussolino (University of Turin, Italy). All these cell lines were cultured in Dulbecco's Modified Eagle's Medium (DMEM) supplemented with 10% FCS (Mascia Brunelli, Milan, Italy), 1.0 mM glutamine and antibiotics. Rat H9C2 embryos heart myoblasts (A.T.C.C.) were cultured in DMEM supplemented with 10% bovine calf serum, 1.0 mM glutamine and antibiotics. Human MCF7 adenocarcinoma cells (A.T.C.C.) were cultured in F-12 Ham with 25 mM HEPES and $NaHCO_3$ supplemented with 10% FCS, 1.0 mM glutamine and antibiotics. All cell cultures were maintained and used for experiments at approximately 90% confluence in a 5% CO_2 humidified atmosphere at 37°C. Cells were used for a maximum of 20 passages.

Aliquots of solutions containing native or aggregated protein in prefibrillar or fibrillar forms were centrifuged, dried under N_2 to remove the TFE when necessary, dissolved in the appropriate cell media at 200 μM concentration and immediately added to cultured cells at differing final concentrations. Protein concentration in the aggregates is that of the soluble monomer. Cells were incubated in the presence of the aggregates for 24 hours; in some cases, cells were exposed to the aggregates for differing lengths of time. Previous data indicate that, under our conditions, HypF-N pre-fibrillar aggregates are mainly present as small globular particles or beaded chains of partially unfolded monomers or oligomers (Bucciantini et al., 2002; Relini et al., 2004). No depolimerization and microscopic difference in aggregate structures were observed following dilution in the cellular culture media.

Assay of cell viability

The cytotoxicity of the HypF-N aggregates was assessed by the 3-(4,5-dimethylthiazol-2-yl)-2,5-diphenyltetrazolium bromide (MTT) assay. Cells were plated on 96-well plates in 100 μl of fresh medium. After 24 hours, the media were changed with 100 μl of fresh media supplemented with 2.0 μM (for all cell types) or with differing concentrations (0.2, 2.0 or 20 μM for Hend cells) of pre-fibrillar or fibrillar HypF-N aggregates. In some experiments, Hend cells were pre-treated for 2 hours with 500 μM water-soluble cholesterol (polyoxyethanyl-cholesteryl sebacate) to enrich the cholesterol content of the plasma membrane, washed with cholesterol-free media and supplemented with HypF-N aggregates. After 24 hours, 100 μl of MTT solution in PBS was added to the cell cultures (0.5 mg ml^{-1} final concentration) and samples were incubated at 37°C for 4 hours. 100 μl of cell lysis buffer (20% SDS, 50% N,N-dimethylformamide, pH 4.7) was added to each well and the samples were incubated overnight at 37°C in a humidified incubator. Absorbance values of blue formazan were determined at 590 nm with an automatic plate reader.

Assay of the cholesterol content in cell surface membrane

Cholesterol in the surface membrane of untreated cells was assayed as previously described (Lange and Ramos, 1983). Briefly, 2.0×10^6 cells were washed twice and resuspended in 300 μl of phosphate buffer, pH 7.5, containing 310 mM sucrose. The cells were incubated at 37°C for 2 hours with cholesterol oxidase (2.5 U ml^{-1}) and phospholipase C (0.2 U ml^{-1} in 1.3 mM $CaCl_2$) to make cholesterol in the intact membranes available for cholesterol oxidase (Moore et al., 1977). Then, 600 μl of Dole Reagent (470 μl isopropanol, 120 μl heptane, 12 μl H_2O) was added to the reaction mixture, followed by 300 μl of heptane to terminate the reaction and to reduce the background by lipid extraction. Total oxidized cholesterol was assayed as cholest-4-en-3-one, after vortexing and centrifuging 10 minutes 2000 ***g*** at 4°C, in the upper phase at 235 nm. Controls consisted of cells supplemented with all the reagents except cholesterol oxidase. Cholesterol content was determined by comparison with a reference curve built by assaying differing amounts (1-50 μg) of cholesterol dissolved in 15 μl of isopropanol.

Time-course of HypF-N aggregate binding to cell surface membrane

Cells treated for differing times (0, 5, 10, 15, 20, 30, 60 minutes) with 2.0 μM HypF-N pre-fibrillar aggregates in a 96-well plate were washed twice with PBS. The residual aggregate-cell complex was stained with 100 μl of 2.0 μM Congo Red in PBS for 20 minutes. The Congo Red content was measured photometrically at 490 nm (free Congo Red) and 550 nm (bound Congo Red) with an ELISA plate reader. Under these conditions, the optical density at 550 nm of the HypF aggregate-Congo Red complex is a measure of the amount of pre-fibrillar aggregates adsorbed to the cell membrane (Datki et al., 2004).

Measurement of intracellular ROS

Cells were cultured in 6-well plates in 2.0 ml of fresh medium. Intracellular ROS levels were detected in cells exposed 3 or 24 hours to 2.0 μM HypF-N pre-fibrillar aggregates by using 5.0 mM ROS-sensitive fluorescent probe DCFH-DA. Cells were washed twice with PBS and lysed with RIPA buffer (50 mM Tris/HCl, 150 mM NaCl, 1.0% Triton X-100, 100 mM NaF, 2.0 mM EGTA, 1.0 mM vanadate, pH 7.5) containing 0.1 mM PMSF, 10 μg ml^{-1} leupeptin and 10 μg ml^{-1} aprotinin. Fluorescence was measured using a Perkin Elmer LS 55 spectrofluorimeter at 480 nm excitation and 530 nm emission wavelengths. Untreated cells were used for background readings.

DCFH-DA fluorescence into intact cells was also detected by using a confocal Bio-Rad MCR 1024 ES scanning microscope (Bio-Rad, Hercules, CA) equipped with a krypton/argon laser source (15 mW). A series of optical sections (512×512 pixels) was taken through the depth of the cells with a thickness of 1.0 μm at intervals of 0.8 μm. Twenty optical sections for each examined sample were then projected as a single composite image by superimposition. Cells were cultured on glass coverslips and at differing times of exposure to the aggregates, dye loading was achieved by incubating the cells with DCFH-DA for 20 minutes at 37°C in the culture medium. Then the cells on coverslips were fixed with 2.0% paraformaldehyde for 10 minutes, mounted on glass and analyzed by the confocal microscope.

Cell lysis

Cells were washed twice in PBS, and dissolved in 50 mM Tris-HCl buffer, pH 7.2 containing 0.1 mM PMSF, 10 μg ml^{-1} leupeptin and 10 μg ml^{-1} aprotinin prior to storage at –80°C until use. Rupture of the plasma membrane was achieved by three freeze-thaw cycles followed by centrifugation at 750 ***g*** for 10 minutes at 4°C. The pellet containing the nuclear fraction was resuspended in 20 mM HEPES buffer, pH 7.4, containing 250 mM sucrose, 2.0 mM EGTA, 1.0 mM EDTA, and sonicated twice (5 seconds each time) in ice. Protein content was measured in cytosolic and nuclear fractions according to the method of Bradford (Bradford, 1976).

Assay of total antioxidant capacity

The total antioxidant capacity (TAC), accounting for total hydrophilic scavengers, was assayed in cytosolic fractions of cell lysates by a spectrophotometric method (Total Antioxidant Status, Randox Laboratories LTD., Co. Antrim, UK). In brief, 2,2′-azino-di-[3-ethylbenzthiazoline sulfonate] (ABTS) was incubated with a

peroxidase (metmyoglobin) and H_2O_2 to generate the blue-green radical cation $ABTS^{\bullet+}$ with maximum absorbance at 600 nm. $ABTS^{\bullet+}$ is reduced in the presence of antioxidants as a function of the concentration of the latter. The results were calibrated using a reference curve based on the soluble antioxidant Trolox (6-hydroxy-2,5,7,8-tetramethylchroman-2-carboxylic acid) as a standard.

Measurement of lipid peroxidation products

To assess the rate of lipid peroxidation, the levels of typical end products of the process, such as MDA and 4-HNE, were determined in the cytosolic fraction of cellular lysates obtained as described above. Measurements were made by using a colorimetric method at 586 nm, according to the reaction of the chromogen N-methyl-2-phenylindole, with MDA and 4-HNE in the presence of methanesulfonic acid at 45°C (Esterbauer et al., 1991).

Intracellular free Ca^{2+} determination

Free cytosolic Ca^{2+} was measured by the procedure of Grynkiewicz et al. (Grynkiewicz et al., 1985). Briefly, cells exposed to the HypF-N aggregates were loaded with 10 μM Fura2-AM using a 1000× solution in anhydrous DMSO previously mixed 1:1 with 20% Pluronic acid F127. Incubation was carried out at 37°C for 60 minutes; then the cells were washed twice with PBS to remove the excess dye, gently trypsinized, centrifuged and washed with a large excess of 10 mM MOPS, pH 7.0, containing 115 mM KCl, 20 mM NaCl, 1.0 mM EGTA and 1.0 mM $MgCl_2$. Cells were resuspended in 100 μl of 10 mM MOPS buffer, pH 7.0, containing 115 mM KCl, 20 mM NaCl, 10 mM EGTA and 1.0 mM $MgCl_2$ and diluted to a final volume of 2.0 ml in a thermostated spectrofluorimeter cuvette. All operations were carried out at 25°C. Intracellular calcium concentration was calculated as previously reported (Bucciantini et al., 2004). The volume of added samples was no more than 0.2% of the cuvette volume.

Confocal analysis of calcium transients

The modifications of the intracellular Ca^{2+} concentrations in Hend and HeLa cells incubated with HypF-N aggregates were monitored in cells plated on glass coverslips and incubated at RT for 10 minutes in serum-free DMEM containing 0.1% BSA, 10 μM (final concentration) Fluo3-AM as fluorescent calcium indicator, 0.1% DMSO and Pluronic acid F-127 (0.01% w/v). Then the cells were washed and maintained in fresh medium for 10 minutes to allow complete Fluo-3 hydrolysis and placed in open slide flow-loading chambers mounted on the stage of a confocal Bio-Rad MRC 1024 ES scanning microscope. Cell fluorescence was monitored at 488 nm excitation by collecting the emitted fluorescence with a Nikon Plan Apo ×60 oil-immersion objective through a 510 nm long-wave pass filter. The time course analysis of Ca^{2+} waves after stimulation with 2.0 μM HypF-N pre-fibrillar aggregates was performed with Time Course Kinetic software (Bio-Rad). Usually, cells did not reach confluence on coverslips; a single coverslip with adherent cells was used for only one experiment. For each experiment, a variable number of cells ranging from 10 to 22 were analyzed. Fluorescence signals are expressed as fractional changes above the resting baseline, $\Delta F/F$, where F is the average baseline fluorescence before the application of HypF-N and ΔF represents the fluorescence changes over the baseline.

In a separate set of experiments, intracellular free Ca^{2+} was imaged at differing times of cell exposure to the aggregates; cells were incubated with 10 μM Fluo3-AM for 10 minutes, fixed with 2.0% paraformaldehyde for 10 minutes, mounted on glass and analyzed on the confocal microscope.

Ca^{2+}-ATPase and ATP assays

The activity of Ca^{2+}-ATPase was measured in membrane fractions obtained from cell lysates as reported above by a coupled optical assay at 340 nm and 37°C. Culture media contained 10 mM HEPES buffer, pH 7.0, 100 mM KCl, 5.0 mM $MgCl_2$, 1.0 mM EGTA, 2.0 mM NaN_3, 0.5 mM phosphoenolpyruvate, 0.2 mM NADH, 1.0 mM ATP, 10 units of PK, 14 units of LDH and 100 μg of membrane proteins. Measurements were carried out in the presence of 2.0 mM ouabain to inhibit the Na^+,K^+-ATPase activity. Ca^{2+}-ATPase activity, expressed as nmol of ATP hydrolyzed min^{-1} mg^{-1} membrane proteins, was calculated as the difference of ATP hydrolysis in the presence and in the absence of 5.0 mM $CaCl_2$ to exclude the contribution of ATPase activities other than the Ca^{2+}-ATPase (Saborido et al., 1999).

ATP measurements were performed by a highly sensitive bioluminescence assay (Kit HS II, Roche Diagnostics, Mannheim, Germany) based on the ATP-dependence of the light emitting oxidation of luciferin catalyzed by luciferase (Lundin, 2000).

Apoptotic and necrotic markers

LDH release was measured in the culture media of cells exposed 24 hours to the aggregates by a routine spectrophotometric test at 340 nm. DNA fragmentation, accounting for cell apoptosis, was determined by an immunometric method (Cell Death Detection ELISA^{PLUS}, Roche Diagnostics) according to the manufacturer's instructions. DNA fragmentation was expressed as the enrichment of histone-associated mono- and oligonucleosomes released to the cytoplasm by measuring the absorption at 405 nm.

Caspase-3 cleavage in the cytosolic fractions, obtained as previously described, was measured after 15% SDS-PAGE run of 50 μg proteins. The gels were blotted on PVDF Immobilon-P Transfer Membrane and probed by overnight incubation with rabbit anti caspase-3/CPP32 polyclonal antibodies followed by incubation with the HRP-conjugated secondary antibody and ECL. Band densities of either the 17 kDa active fragment or the 32 kDa inactive precursor were measured as densitometric units per μg protein using the image analysis and densitometry program Quantity One (BioRad, Milan, Italy).

Nuclear and mitochondrial fractions were used to assess Bcl-2 and PARP compartmentalization in Hend and HeLa cells. Subcellular fractionation was achieved using the cytosol/mitochondria fractionation kit and homogenized samples were treated as indicated by the manufacturer. The cleaved fragment of either the nuclear PARP (89 kDa) or the mitochondrial Bcl-2 (25 kDa) were determined by 12% SDS-PAGE and western blotting using C2-10 anti-PARP and anti-Bcl-2 monoclonal antibodies, respectively, followed by anti-mouse secondary antibodies. For each band of interest, control values were taken as 100% and values relative to HypF-N treated cells were calculated as a percentage of the control within the same blot.

Statistical analysis

The results were examined by Pearson bivariate correlations and individual group means compared with Bonferroni's test. A P value <0.05 was set as significant.

Results

Pre-fibrillar aggregates are much more toxic than mature fibrils in all investigated cell types

All investigated cell types exposed for 24 hours to 2.0 μM HypF-N pre-fibrillar aggregates displayed significantly reduced viability, as measured by the MTT test. However, the extent of cell impairment was different in the various cell types, leading us to rank cells according to their susceptibility; Hend cells were the most heavily affected whereas IMR90 and HeLa were the most resistant (Fig. 1). In all investigated cell types, a strict correlation between cell viability and the amount of

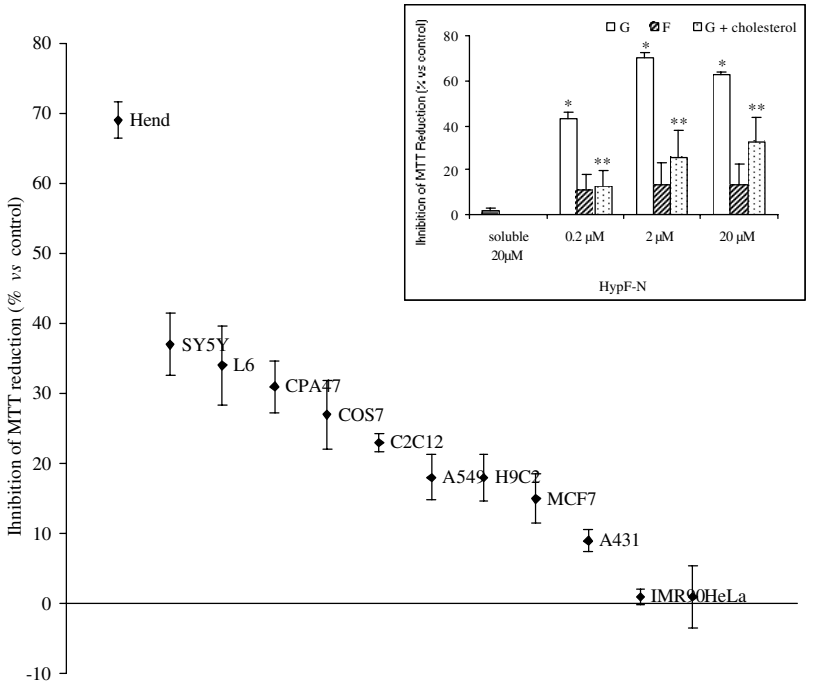

Fig. 1. Various cell lines are differently affected by pre-fibrillar aggregates. Cell viability was checked by the MTT test, after supplementing cell culture media with 2.0 μM HypF-N pre-fibrillar aggregates. Values are relative to control cells treated with the soluble HypF-N (means ±s.d.). The inset shows the percentage of cell death in the most susceptible cell type (Hend) exposed to varying amounts of fibrillar (F) or pre-fibrillar (G) aggregates. Hend cells were pre-treated to enrich the cholesterol content of the plasma membrane before exposure to pre-fibrillar aggregates (G+cholesterol). For technical details see under Materials and Methods. The reported values are representative of six independent experiments, each performed in duplicate. *$P \leq 0.05$, significant difference *vs* cells exposed to the soluble HypF-N. **$P \leq 0.05$, significant difference *vs* not pre-treated cells exposed to the HypF-N pre-fibrillar aggregates.

aggregates added to the culture media was found. In particular, the extent of cell impairment in the most susceptible cell line (Hend) ranged from 43% at the lowest aggregate concentration used (0.2 μM) to 62% at the highest one (20 μM). At all protein concentrations a highly significant decrease of viability was found with respect to control cells exposed to 20 μM monomeric HypF-N (Fig. 1, inset). As the lowest aggregate concentration producing the highest cytotoxic effect was 2.0 μM, all subsequent experiments were carried out using this aggregate concentration.

The extent of MTT reduction was substantially the same in all cell lines exposed to 0.2-20 μM mature fibrils [as exemplified by Hend cells (F) in the inset of Fig. 1]. The slight toxicity of the mature fibrils was likely due to the presence, in the samples, of minute amounts of residual pre-fibrillar aggregates, although a specific, yet moderate, fibril toxicity cannot be ruled out. The low (if any) toxicity of HypF-N mature fibrils to all investigated cell lines confirms previous results concerning two different cell lines, PC-12 and NIH-3T3 (Bucciantini et al., 2002).

Membrane cholesterol content

The role of membrane cholesterol content in the pathogenesis of amyloid diseases is controversial (Ledesma and Dotti, 2005). To our knowledge, there are no data on the possible modulation of aggregate interaction with cell membranes in relation to the proportion of cholesterol in membranes. We investigated whether a significant correlation between cholesterol content in the plasma membranes and cell viability could be established following cell exposure to HypF-N pre-fibrillar aggregates for 24 hours, as assessed by the MTT test. We found a significant inverse correlation between inhibition of reduction of MTT and membrane cholesterol (Table 1).

To assess further the role of membrane cholesterol in improving cell resistance to the aggregates, we determined the susceptibility and/or resistance to the HypF-N aggregates of the most affected cell type (Hend) cultured for 2 hours in the presence of 0.5 mM soluble cholesterol leading to significant enrichment of the amount of membrane cholesterol (125%, $P \leq 0.05$). Fig. 1 (inset) shows the cytotoxicity of varying amounts of HypF-N pre-fibrillar (G) aggregates to Hend cells in the absence or in the presence (G+cholesterol) of cholesterol supplemented to the culture media. It can be seen that cell resistance to the toxic aggregates is highly enhanced following membrane enrichment with cholesterol. This finding was confirmed by assessing the time-course of aggregate binding to Hend (either normal or enriched in membrane cholesterol) and HeLa cells exposed for varying lengths of time to 2.0 μM HypF-N pre-fibrillar aggregates, washed with PBS and finally

Table 1. Correlations between basal biochemical parameters or their modifications in 12 different cell lines exposed 24 hours to pre-fibrillar HypF-N aggregates

	DNA fragmentation	Caspase-3 cleavage	ROS	Cytosolic Ca^{2+}	Membrane cholesterol
MTT	0.54/<0.05*	0.30/>0.05	0.57/<0.05*	0.15/>0.05	–0.56/<0.05*
DNA fragmentation		0.76/<0.01*	0.57/<0.05*	0.22/>0.05	–0.39/>0.05
Caspase-3 cleavage			0.34/>0.05	0.58/<0.05*	–0.16/>0.05
ROS				0.87/<0.001*	–0.29/>0.05
Cytosolic Ca^{2+}					–0.35/>0.05

Correlation coefficient (r) and relative significant values (P) (r/P); *significant values.

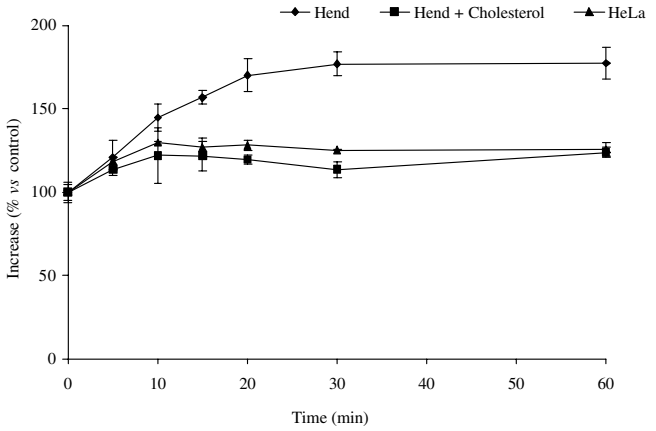

Fig. 2. Time-course of HypF-N binding to HeLa and Hend cells (either normal or enriched in membrane cholesterol). Both cell lines were exposed for 5, 10, 15, 20, 30, 60 minutes to 2.0 μM HypF-N pre-fibrillar aggregates and then washed twice with PBS. The residual aggregate-cell complex was stained with 2.0 μM Congo Red for 20 minutes. Under these conditions, Congo Red-staining is a measure of the amount of prefibrillar aggregates adsorbed to cell membrane surface. Binding of HypF-N aggregates to Hend cell membranes was highly reduced following supplementation of the culture media with 0.5 mM water-soluble cholesterol.

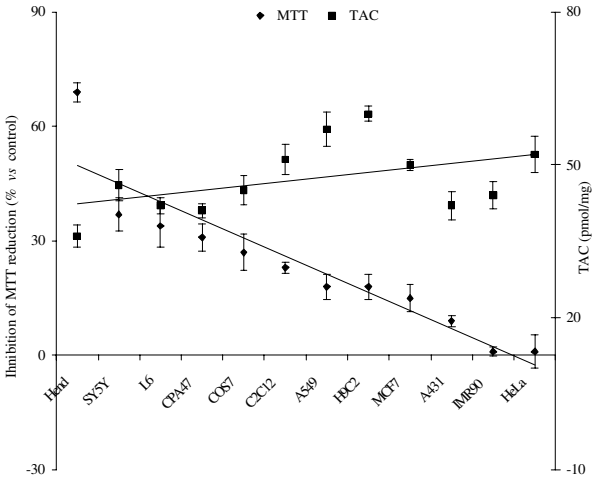

Fig. 3. Correlation between susceptibility and total antioxidant capacity. Basal TAC was correlated with cell viability (as determined by the MTT test) in cells exposed to 2.0 μM aggregated HypF-N for 24 hours. TAC values are expressed as pmol of $ABTS^{\bullet+}$ produced per mg of protein. For technical details see under Materials and Methods. TAC values are the means of three experiments carried out in duplicate.

stained with 2.0 μM Congo Red (Fig. 2). Under these conditions, Congo Red-staining is a measure of the amount of prefibrillar aggregates bound to the cell membrane. It can be seen that, following supplementation of the culture media with water-soluble cholesterol, the binding of HypF-N aggregates to Hend cells was considerably reduced to values almost identical to those displayed by the most resistant cell line (HeLa). This finding supports the idea that, at least in the case of the highly susceptible Hend cells, increasing membrane cholesterol reduces cell susceptibility to the aggregates by impairing the adsorption of the aggregates to the plasma membrane.

Oxidative stress

There is strong experimental evidence suggesting that oxidative stress is one of the early biochemical modifications in cells experiencing toxic pre-fibrillar aggregates (Janciauskiene and Ahrén, 2000; Squier, 2001; Dargusch and Schubert, 2002; Dobson, 2003; Stefani et al., 2003; Bucciantini et al., 2004). It is well known that oxidative stress can be the effect of either any increased free radical production and/or the weakening of the cell antioxidant defences, including antioxidant enzymes, lipophilic and hydrophilic scavengers. We measured, in each cell line, the levels of non-enzymatic hydrophilic TAC, relating it to the different susceptibility to aggregate damage. The investigated cell lines displayed a differing basal TAC, and a significant inverse relation (r=–0.54, P≤0.05) was found between the basal TAC and cell viability, as assessed by the MTT test, following cell exposure for 24 hours to the HypF-N pre-fibrillar aggregates (Fig. 3). A significant correlation was also found in all investigated cell lines between cell viability and ROS levels (Table 1). Indeed, a significant increase in ROS production was found in the differing cell lines exposed to 2.0 μM aggregates for 24 hours respect to controls exposed to the soluble domain. Hend and HeLa, chosen as examples of high and low susceptibility to damage displayed 300% (Hend) and 180% (HeLa) ROS levels respect to controls. These values, although relative to cells exposed to the aggregates for prolonged times, are indicative of a different ability of the variously affected cell lines to counteract the oxidative stress.

The levels of ROS in the two representative cell lines were also measured at early times of exposure by time-course confocal analysis (Fig. 4). An early and sharp increase of

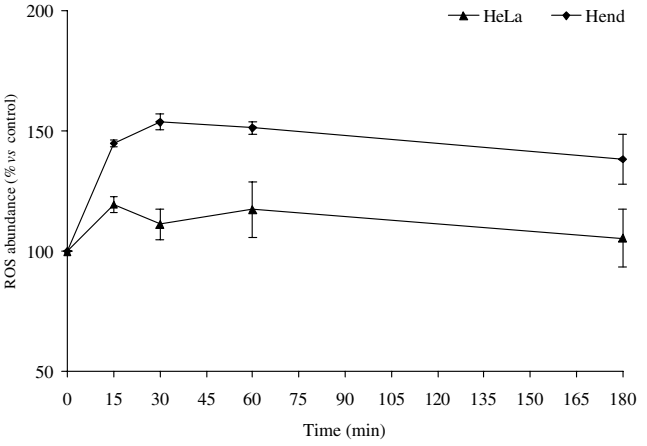

Fig. 4. Time course of ROS accumulation. Confocal microscopy analysis of the redox status of two different cell lines exposed for 15, 30, 60, 180 minutes to 2.0 μM HypF-N pre-fibrillar aggregates. ROS production was checked by incubating the exposed cells, for 10 minutes, in the presence of the redox fluorescent probe CM-H2 DCFA. For technical details see under Materials and Methods. The values shown are means of three experiments carried out in duplicate.

Table 2. Correlations between basal biochemical parameters or their modifications in 12 different cell lines exposed 3 h to pre-fibrillar HypF-N aggregates

	ROS	Ca^{2+}-ATPase	ATP	TAC	Membrane cholesterol
DNA fragmentation	–0.30/>0.05	–0.66/<0.01*	0.05/>0.05	–0.25/>0.05	–0.11/>0.05
ROS		–0.09/>0.05	0.17/>0.05	–0.34/>0.05	–0.60/<0.05*
Ca^{2+}-ATPase			–0.63/<0.05*	0.59/<0.05*	0.35/>0.05
ATP				0.07/>0.05	–0.10/>0.05
TAC					0.37/>0.05

Correlation coefficient (r) and relative significant values (P) (r/P); *significant values.

intracellular ROS can be seen in the most affected cell line (Hend) displaying the lowest TAC value, whereas a much lower increase was found in the most resistant cell line. In Hend cells, the highest increase, in the 15-60 minutes interval, was followed by a slow decrease at prolonged times of exposure. A significant early ROS increase following exposure to HypF-N aggregates has been reported for another cell line (NIH-3T3) displaying low resistance to the toxic effects of the aggregates (Bucciantini et al., 2004). Interestingly, the early ROS increase following exposure for 3 hours to the HypF-N pre-fibrillar aggregates displayed a significant inverse relation with cholesterol content in the surface membrane of each cell type (Table 2). In the two representative cell lines, ROS accumulation resulted in an evident increase in membrane lipoperoxidation (as assessed by measuring the levels of MDA plus 4-HNE) with respect to controls exposed to the monomeric protein (117±7%, Hend; 112±5% HeLa).

Intracellular free Ca^{2+} levels

It is generally reported that differing cell types undergoing oxidative stress display a rapid increase in free Ca^{2+} concentration (reviewed in Gennady and Kelvin, 2001). Previously reported data showed that in NIH-3T3 cells exposed to toxic HypF-N aggregates, a significant intracellular free Ca^{2+} increase occurs after a few minutes of exposure (Bucciantini et al., 2004). We confirmed this finding in all investigated cell lines exposed to the aggregates; in fact, under our experimental conditions, each cell line displayed different increases of the intracellular free Ca^{2+} levels that significantly correlated with ROS increases (Table 1) suggesting that, in each cell type, intracellular free Ca^{2+} and ROS increases can positively affect each other.

The positive correlation between Ca^{2+} and ROS levels is also supported by confocal analysis of he ROS and free Ca^{2+} content in Hend cells exposed to HypF-N aggregates, plated on glass coverslips and fixed at various times of exposure (Fig. 5). It can be seen that the rise of cytosolic free Ca^{2+} was higher than ROS increase but followed similar kinetics; indeed, the free Ca^{2+} level peaked at very early times of exposure (15 minutes), decreased until 3 hours and increased again at later times of exposure, whereas ROS increase was smoother and did not show any early peak.

The time courses of the free intracellular Ca^{2+} levels were also monitored for 20 minutes by confocal microscopy carried out on unfixed, viable Hend and HeLa cells exposed to the aggregates (Fig. 6). The free Ca^{2+} increase in Hend cells was earlier, higher and more prolonged than was the increase found in HeLa cells under the same conditions. These data suggest that the more susceptible and the more resistant cells are provided with a poorly or a highly efficient biochemical machinery aimed at counteracting any uncontrolled free Ca^{2+} increase in the cytosol, respectively.

The possible relationship between susceptibility to damage and calcium pump efficiency was assessed by measuring the total Ca^{2+}-ATPase activity in each cell line of the investigated panel exposed 3 hours to the aggregates (Table 3). A significant negative correlation was found between impairment of cell viability (as assessed by the MTT test) and Ca^{2+}-ATPase activity (r=–0.67, P<0.01). Furthermore, the cell lines endowed with higher TAC levels displayed a higher activation of the Ca^{2+}-pumps (Table 2). These correlations support the idea that the ability to counteract aggregate toxicity may be traced back, at least in part, to the efficiency of the systems aimed at clearing any free Ca^{2+} excess as well as to the resistance of these systems to oxidative inactivation. Moreover, in all cell lines exposed for 3 hours, the increase of Ca^{2+}-ATPase activity displayed a significant inverse relation to intracellular ATP content and DNA fragmentation (and hence to apoptotic pathway activation) (Table 2).

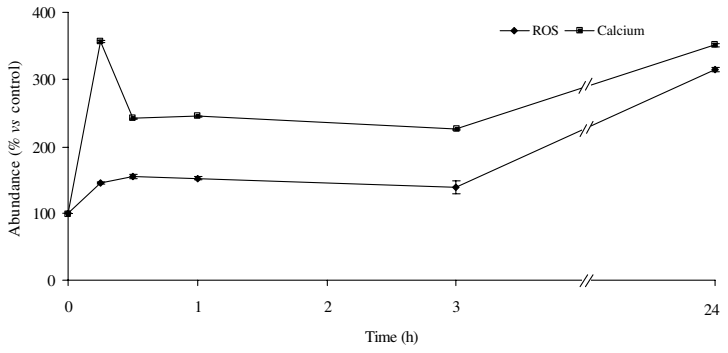

Fig. 5. Changes of intracellular ROS and free Ca^{2+} levels in Hend cells checked by confocal analysis. Cells were exposed for 15, 30, 60, 180 minutes and 24 hours to 2.0 μM HypF-N pre-fibrillar aggregates and then fixed with 2.0% paraformaldehyde. ROS were obtained by incubating for 10 minutes the exposed cells in the presence of the redox fluorescent probe and by measuring the fluorescence of CM-H2 DCFA. Intracellular free Ca^{2+} levels were revealed by incubating the exposed cells for 15 minutes in the presence of the fluorescent dye Fluo-3AM. The data are reported as percentages of the values determined at time 0 and are expressed as means ±s.d. of four experiments each carried out in duplicate. For technical details see under Materials and Methods.

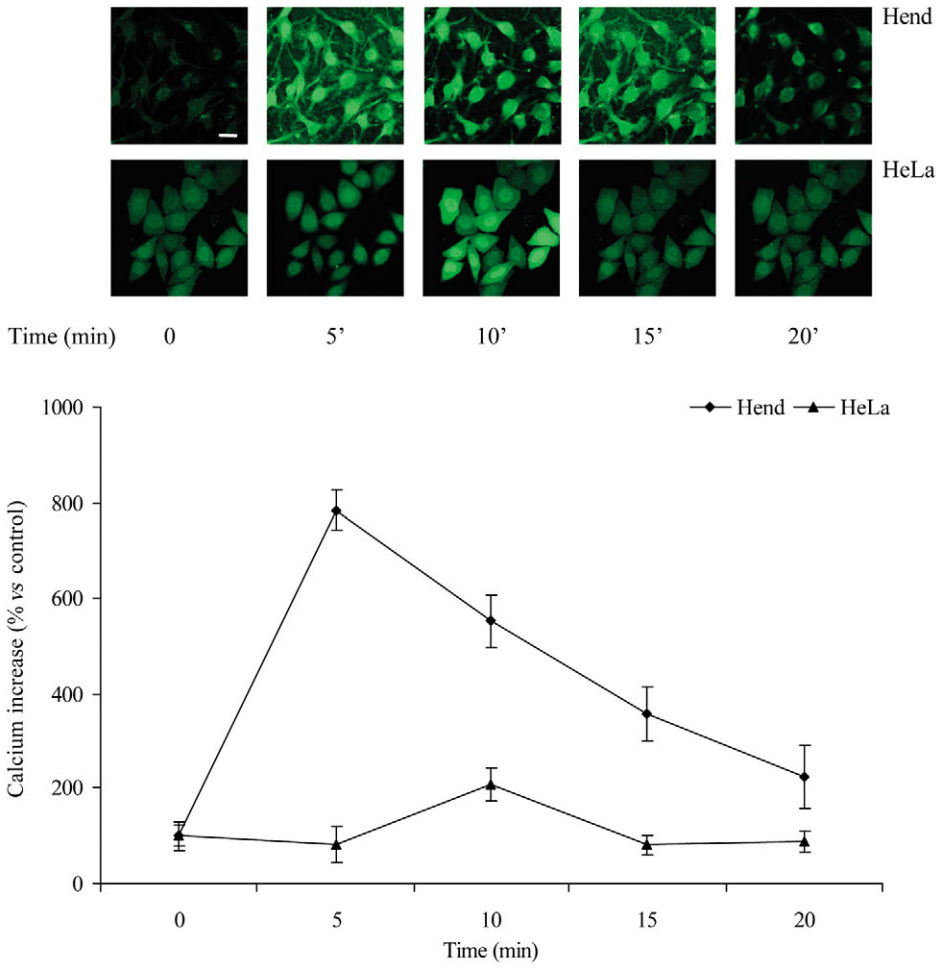

Fig. 6. Continuous confocal microscopy analysis of intracellular free Ca^{2+} levels in unfixed Hend and HeLa cells. Intracellular free Ca^{2+} levels were imaged by confocal microscopy using the fluorescent dye Fluo-3AM as a probe as described under Materials and Methods. Cells were exposed for 20 minutes to 2.0 μM HypF-N aggregates. Fluorescence is expressed as fractional change above the resting baseline, $\Delta F/F$, where F is the average baseline fluorescence before aggregate exposure and ΔF is the fluorescence change over the baseline. The values shown are means ±s.d. of three independent experiments each carried out in triplicate. Bar, 30 μm.

Apoptotic and necrotic markers

In addition to impairing cell viability, HypF-N pre-fibrillar aggregates have previously been found to induce necrotic death in NIH-3T3 cells following early caspase-3 activation (Bucciantini et al., 2004). In all our investigated cell lines (not including NIH-3T3), the aggregate-induced stress was associated with typical apoptotic features, such as DNA fragmentation and caspase-3/CPP32 cleavage, rather than with necrotic markers. In all cell lines, the release of cellular LDH to the culture media was not significantly increased upon 24 hours exposure to the pre-fibrillar aggregates with respect to controls incubated with the monomeric domain; also it did not significantly correlate with cell viability (r=0.004, P>0.05), further supporting the absence of a necrotic outcome in the exposed cell lines.

By contrast, the amount of histone-associated oligonucleosomes released to the cytoplasm was indicative of a significant increase of DNA fragmentation in nearly all investigated cell lines exposed to the HypF-N aggregates for 24 hours (Table 3). DNA fragmentation displayed a significant positive correlation with the impairment of cell viability and with the increases of either ROS or the active caspase-3 fragment, a typical late apoptotic marker (Table 1). Interestingly, the cell line most heavily affected by the aggregates (Hend) displayed an early slight rise of DNA fragmentation reaching about 160% at 3 hours exposure.

Table 3. Effects on Ca^{2+}-ATPase activity and DNA fragmentation elicited in 12 different cell lines after 3 hours and 24 hours exposure, respectively, to HypF-N pre-fibrillar aggregates

	Ca^{2+}-ATPase (3 h)	DNA fragmentation (24 h)
Hend	150±23%	224±35%
SH-SY5Y	118±19%	92±18%
L6	110±18%	135±23%
CPA47	125±20%	90±20%
COS7	200±27%	123±15%
C2C12	280±35%	211±30%
A549	206±30%	106±6%
H9C2	270±32%	112±12%
MCF7	275±44%	125±16%
A431	228±38%	97±14%
IMR90	250±26%	116±18%
HeLa	266±39%	129±20%

The data are reported as a proportion of the value determined in untreated cells (taken as 100%) and are means ±s.d.% of three independent experiments.

Ca^{2+} levels regulate many biological functions including apoptosis; indeed, it is well known that Ca^{2+} release from the

Table 4. Apoptotic markers in two cell lines carrying different grade of susceptibility

Marker	Susceptible (Hend)	Resistant (HeLa)
Bcl-2 (M) 25 kDa	25±8%	203±37%
PARP fragment (N) 89 kDa	169±39%	165±35%
Caspase-3 (C) 32 kDa	48±11%	80±12%

M, mitochondrial fraction; N, nuclear fraction; C, cytosolic fraction. The data are reported as a proportion of the value determined in untreated cells (taken as 100%) and are means ±s.d.% of three independent experiments.

intracellular stores plays a critical role in modulating the activity of caspase-3/CPP32, whose activated form can, in turn, affect free Ca^{2+} levels by cleaving membrane calcium pumps (Tantral et al., 2004). Our results confirmed such a close cross-dependence; in fact, following 24 hours exposure to the aggregates, all investigated cell lines displayed a positive correlation between the rise of free Ca^{2+} and the content of the caspase-3 active fragment (Table 1). The results concerning the pro-apoptotic effector caspase-3/CPP32 also agreed with the susceptibility scale. In fact, the inactive precursor of caspase-3 was less abundant in the most affected cell line suggesting a higher presence of its active, truncated form.

The apoptotic process was further investigated by measuring the levels of some typical anti- and pro-apoptotic markers in highly susceptible (Hend) or highly resistant (HeLa) cells exposed for 3 hours. The anti-apoptotic factor Bcl-2 was significantly decreased in Hend cells, whereas it was upregulated in HeLa cells (Table 4). Another pro-apoptotic marker, PARP cleavage activation, although similar in both cell lines confirmed the observed apoptotic pattern.

Discussion

To our knowledge, the biochemical features determining the different susceptibility of various cell types to the toxic effects of amyloids have not yet been investigated in detail. Our study sought to provide information on this topic by exposing a panel of normal or pathological cell lines to toxic pre-fibrillar aggregates of HypF-N, a protein not associated with any amyloid disease, previously shown to display the same structural features and properties of the aggregates produced by disease-associated peptides and proteins (Relini et al., 2004). Previous reports have shown that pre-fibrillar aggregates of proteins not associated with disease are toxic to cells in a manner similar to early aggregates of disease-related proteins and peptides (Bucciantini et al., 2002; Kranenburg et al., 2003; Sirangelo et al., 2004) by impairing the same biochemical parameters (Bucciantini et al., 2004). Under our experimental conditions, differing cell lines were variously affected by the same amount of toxic prefibrillar aggregates of a particular protein, whereas mature fibrils were substantially non-toxic; this finding suggests that the severity of cell impairment was related to the different ability of any cell line to counteract the biochemical modifications resulting from exposure to the aggregates.

It is widely accepted that, at least in most cases, cell degeneration in amyloid diseases is mediated by a toxic mechanism involving the interaction of the aggregated species with the plasma membrane of the affected cells (Kagan et al., 2004). Some authors suggest that, by affecting plasma membrane fluidity, cholesterol content affects the incorporation of toxic aggregates into the plasma membrane itself (Arispe and Doh, 2002). We have found that cholesterol content in the surface membrane of untreated cells displayed a significant positive relation with cell resistance to the toxic insult given by HypF-N pre-fibrillar aggregates. Indeed, in the case of the most susceptible cell type, we found a close relation between content of membrane cholesterol and amount of toxic aggregates adsorbed to the plasma membrane. Furthermore, the amount of surface-bound aggregates was higher in the most susceptible Hend cells, which had a lower membrane cholesterol content, than in the most resistant HeLa cells, which were more rich in membrane cholesterol. Interestingly, Hend cells enriched in plasma membrane cholesterol showed enhanced survival; in these, aggregate absorption to the cell membrane was reduced at levels comparable with those displayed by the most resistant cell type (HeLa). These data agree with the idea that membrane lipid composition is a key biochemical feature affecting aggregate interaction with cells, as well as affecting the type and the extent of the cell's response to their presence; they also further support the widely accepted idea that membrane derangement is an early key step in the path of cell death (Kourie and Henry, 2002; Kagan et al., 2004). In some amyloid diseases, the toxic aggregates are produced inside the cell and do not interact with the outer surface of the plasma membrane, nevertheless, our finding that toxic aggregates display reduced absorption to cell membranes enriched in cholesterol adds new information to the complex relationships between blood cholesterol and susceptibility to neurodegenerative diseases.

Previous reports have highlighted the key role of a number of biochemical parameters, such as redox status, energy load and free Ca^{2+} levels in cells experiencing toxic aggregates of peptides and proteins either associated with amyloid diseases (Mattson, 1999; Kruman et al., 1999; Kawahara et al., 2000; Squier, 2001; Milhavet and Lehmann, 2002; Hyun et al., 2002; Stefani and Dobson, 2003) or not (Bucciantini et al., 2004). Therefore, we investigated whether the different resistance to aggregate toxicity could be traced back to the presence of specific biochemical features affecting such parameters in differing cell lines exposed to the same amount of pre-fibrillar aggregates of the same protein under identical experimental conditions.

In all cell lines exposed to the aggregates for 24 hours, a significant positive correlation was found among ROS increase, cell impairment and DNA fragmentation, and a negative correlation between cell impairment and TAC levels. An early ROS increase was found in the most susceptible cell line (Hend) whereas it was reduced and delayed in the most resistant one (HeLa). These data indicate that some modification of the intracellular redox status did occur in all exposed cell lines, further underscoring its key role in cell impairment. The negative relationship between TAC and cell impairment confirmed the importance of any alteration of the intracellular redox status respect to the susceptibility to damage. Finally, the positive correlation between ROS and DNA fragmentation indicates that the modification of the intracellular redox status is a key event, even with regard to the final apoptotic outcome of our exposed cells.

In general, it is not known why cells exposed to the toxic aggregates undergo ROS increase, although several hypotheses

have been put forward (Butterfield et al., 2001; Milhavet and Lehmann, 2002; Mattson and Liu, 2002; Kanski et al., 2002; Bucciantini et al., 2004). The idea that oxidative stress may be a consequence of the early increase of free Ca^{2+}, due to plasma membrane permeabilization by the aggregates, has recently gained support (Squier, 2001; Kourie and Henry, 2002; Orrenius et al., 2003; Relini et al., 2004). The increase in the intracellular free Ca^{2+} may speed up the oxidative metabolism by activating the dehydrogenases of the Krebs cycle (Squier, 2001) leading to ROS increase. Such an increase in ROS would oxidize membrane proteins and lipids, calmodulin and other proteins with possible impairment of the activity of membrane pumps (Squier, 2001), further increase in free Ca^{2+} and caspase-3 cleavage. The ability of the activated caspase-3 to degrade the Ca^{2+}-ATPase would, in turn, reinforce the increase in free Ca^{2+}, with its translocation inside the mitochondria, release of pro-apoptotic factors and activation of caspase-9, eventually targeting the cell to the apoptotic death (Orrenius et al., 2003).

In this scenario, it is conceivable that cells endowed with a higher basal Ca^{2+}-ATPase activity and TAC are more resistant to any free calcium increase and to the consequent biochemical modifications. Indeed, in our cells we found that the basal Ca^{2+}-ATPase activity was positively correlated with cell viability and negatively correlated with DNA fragmentation and ATP levels. A positive correlation between cytosolic Ca^{2+} levels and caspase-3 cleavage was also found in all cell lines. Taken together, these data indicate that, in all investigated cell lines, the interaction of pre-fibrillar aggregates with the cells modifies membrane permeability and ion balance leading to activation of either the oxidative metabolism and/or the apoptotic pathway.

The involvement of Ca^{2+} in cell life and death is very complex and not yet well understood. It is known that a large elevation of Ca^{2+} concentration initiates several self-destructive cellular pathways comprising free radical production, activation of catabolic enzymes and derangement of structure and function of cellular organelles (Ferrari et al., 2002). Subtle changes in the mechanisms controlling cellular Ca^{2+} homeostasis can also have profound effects onto the decision between life and death (Ferrari et al., 2002). Indeed, in the most susceptible cell line (Hend) the increase in free Ca^{2+} displayed an early peak after 15 minutes exposure, followed by a decrease (although not reaching the basal level) and by a further increase after 3 hours. Such an early increase was not seen in the more resistant cell line possibly due to its higher basal Ca^{2+}-ATPase activity; however, the possibility that the plasma membranes of these cells are more resistant to the destabilizing effect of the aggregates cannot be ruled out, as suggested by their higher content in cholesterol and by their reduced tendency to interact with the toxic aggregates. The free Ca^{2+} increase found in Hend cells at later times of exposure can be the consequence of the impairment of membrane pumps following concurrent increase in ROS, as confirmed by other oxidative markers such as MDA plus 4-HNE.

After 24 hours exposure to the aggregates, all investigated cell lines died by apoptosis. We have not investigated in detail the features of the apoptotic pathway triggered under these conditions; however, in the two cell lines chosen as representative of high or low susceptibility to the aggregates, a significant negative correlation was found between susceptibility and levels of either Bcl-2, a well known anti-apoptotic factor, and the inactive precursor of caspase-3, as assessed by measuring caspase-3 decrease. PARP fragmentation data further confirmed that the apoptotic cascade was triggered by the pre-fibrillar aggregates in all cell lines. These data agree with previously reported findings indicating a link between Bcl-2 and Ca^{2+} levels in cell compartments (Pinton et al., 2000).

Overall, our data confirm the idea that membrane destabilization by the aggregates and the subsequent early modifications of ion balance and intracellular redox status may trigger subsequent modifications eventually leading to cell death (Mattson, 1999; Kruman et al., 1999; Kawahara et al., 2000; Gennady and Kelvin, 2001; Milhavet and Lehmann, 2002; Hyun et al., 2002; Mattson and Liu, 2002; Kayed et al., 2003; Tantral et al., 2004; Bucciantini et al., 2004; Bucciantini et al., 2005). In this context, we have found that membrane cholesterol may play a key role in disfavouring aggregate absorption to the plasma membrane thus triggering the cascade of events eventually leading to cell death. Our data also indicated that aggregate adsorption, and hence cell susceptibility to damage by the aggregates, is significantly correlated with the levels of anti-oxidant defences, the efficiency of the Ca^{2+} pumps and the expression of apoptotic factors. Therefore, membrane lipid composition and the efficiency of the biochemical equipment aimed at counteracting early modifications of the intracellular ion homeostasis and redox status appear key factors in determining the resistance of exposed cells against the toxic insult given by the aggregates.

In conclusion our data indicate the central role of early membrane derangement in aggregate toxicity by using a panel of differing cell types. Nevertheless, it cannot be excluded that other elements, such as the efficiency of the ubiquitin-proteasome pathway and the levels of molecular chaperones (Sherman and Selkoe, 2001) or the stage of the cell cycle may be equally important with regard to cell susceptibility to protein aggregate toxicity.

We thank Silvia Cappadona for technical advice. This study has been supported by grants from the Italian MIUR (project numbers 2003054414_002, 2002058218_001 and RBNE01S29H_004), the Compagnia di San Paolo, Torino, Italy (ref. 2004.0995) and from the Ente Cassa di Risparmio di Firenze (ref. 2003.1012).

References

Abad-Rodriguez, J., Ledesma, M. D., Craessaerts, K., Perga, S., Medina, M., Delacourte, A., Dingwall, C., De Strooper, B. and Dotti, C. G. (2004). Neuronal membrane cholesterol loss enhances amyloid peptide generation. *J. Cell Biol.* **167**, 953-960.

Abramov, A. Y., Canevari, L. and Duchen, M. R. (2004). Calcium signals induced by amyloid β peptide and their consequences in neurons and astrocytes in culture. *Biochim. Biophys. Acta* **1742**, 81-87.

Arispe, N. and Doh, M. (2002). Plasma membrane cholesterol controls the cytotoxicity of Alzheimer's disease AβP (1-40) and (1-42) peptides. *FASEB J.* **16**, 1526-1536.

Bhagat, Y. A., Obenaus, A., Richardson, J. S. and Kendall, E. J. (2002). Evolution of β-amyloid induced neuropathology: magnetic resonance imaging and anatomical comparisons in the rodent hippocampus. *Magn. Reson. Mater. Phy.* **14**, 223-232.

Bloom, G. S., Ren, K. and Glabe, C. G. (2005). Cultured cell and transgenic mouse models for tau pathology linked to β-amyloid. *Biochim. Biophys. Acta* **1739**, 116-124.

Bokvist, M., Lindstrom, F., Watts, A. and Grobner, G. (2004). Two types

of Alzheimer's beta-amyloid (1-40) peptide membrane interactions: aggregation preventing transmembrane anchoring versus accelerated surface fibril formation. *J. Mol. Biol.* **335**, 1039-1049.

Bradford, M. M. (1976). A rapid and sensitive method for the quantification of microgram quantities of protein utilizing the principle of protein dye binding. *Anal. Biochem.* **72**, 248-254.

Bucciantini, M., Giannoni, E., Chiti, F., Baroni, F., Formigli, L., Zurdo, J., Taddei, N., Ramponi, G., Dobson, C. M. and Stefani, M. (2002). Inherent toxicity of aggregates implies a common mechanism for protein misfolding diseases. *Nature* **416**, 507-511.

Bucciantini, M., Calloni, G., Chiti, F., Formigli, L., Nosi, D., Dobson, C. M. and Stefani, M. (2004). Pre-fibrillar amyloid protein aggregates share common features of cytotoxicity. *J. Biol. Chem.* **279**, 31374-31382.

Bucciantini, M., Rigacci, S., Berti, A., Pieri, L., Cecchi, C., Nosi, D., Formigli, L., Chiti, F. and Stefani, M. (2005). Patterns of cell death triggered in two different cell lines by HypF-N prefibrillar aggregates. *FASEB J.* **19**, 437-439.

Butterfield, A. D., Drake, J., Pocernich, C. and Castegna, A. (2001). Evidence of oxidative damage in Alzheimer's disease brain: central role for amyloid β-peptide. *Trends Mol. Med.* **7**, 548-554.

Caughey, B. and Lansbury, P. T. (2003). Protofibrils, pores, fibrils, and neurodegeneration: separating the responsible protein aggregates from the innocent bystanders. *Annu. Rev. Neurosci.* **26**, 267-298.

Chiti, F., Bucciantini, M., Capanni, C., Taddei, N., Dobson, C. M. and Stefani, M. (2001). Solution condition can promote formation of either amyloid protofilaments or mature fibrils from the HypF N-terminal domain. *Protein Sci.* **10**, 2541-2547.

Dargusch, R. and Schubert, D. (2002). Specificity of resistance to oxidative stress. *J. Neurochem.* **81**, 1394-1400.

Datki, Z., Papp, R., Zadori, D., Soos, K., Fulop, L., Juhasz, A., Laskay, G., Hetenyi, C., Mihalik, E., Zarandi, M. et al. (2004). In vitro model of neurotoxicity of Abeta 1-42 and neuroprotection by a pentapeptide: irreversible events during the first hour. *Neurobiol. Dis*. **17**, 507-515.

Dobson, C. M. (2003). Protein folding and misfolding. *Nature* **426**, 884-890.

Esterbauer, H., Schaur, R. J. and Zollner, H. (1991). Chemistry and biochemistry of 4-hydroxynonenal, malonaldehyde and related aldehydes. *Free Radic. Biol. Med.* **11**, 81-128.

Ferrari, D., Pinton, P., Szabadkai, G., Chami, M., Campanella, M., Pozzan, T. and Rizzuto, R. (2002). Endoplasmic reticulum, Bcl-2 and Ca^{2+} handling in apoptosis. *Cell Calcium* **32**, 413-420.

Gennady, E. and Kelvin, J. A. D. (2001). Calcium and oxidative stress: from cell signaling to cell death. *Mol. Immunol.* **38**, 713-721.

Green, J. D., Kreplak, L., Goldsbury, C., Li Blatter, X., Stolz, M., Cooper, G. S., Seelig, A., Kistler, J. and Aebi, U. (2004). Atomic force microscopy reveals defects within mica supported lipid bilayers induced by the amyloidogenic human amylin peptide. *J. Mol. Biol.* **342**, 877-887.

Grynkiewicz, G., Poenie, M. and Tsien, R. Y. (1985). A new generation of Ca^{2+} indicators with greatly improved fluorescence properties. *J. Biol. Chem.* **260**, 3440-3450.

Hohmann, C., Antuono, P. and Coyle, J. T. (1988). Basal forebrain cholinergic neurons and Alzheimer's disease. In *Handbook of Psychopharmacology: Psychopharmacology of the aging nervous system* (ed. L. L. Iversen and S. H. Snyder), pp. 69-106. Plenum Press, New York.

Hyun, D. H., Lee, M. H., Hattori, N., Kubo, S. I., Mizuno, Y., Halliwell, B. and Jenner, P. (2002). Effect of wild-type or mutant parkin on oxidative damage, nitric oxide, antioxidant defenses, and the proteasome. *J. Biol. Chem.* **277**, 28572-28577.

Iijima, K., Liu, H. P., Chiang, A. S., Hearn, S. A., Konsolaki, M. and Zhong, Y. (2004). Dissecting the pathological effects of human Aβ40 and Aβ42 in *Drosophila*: a potential model for Alzheimer's disease. *Proc. Natl. Acad. Sci. USA* **101**, 6623-6628.

Janciauskiene, S. and Ahrén, B. (1998). Different sensitivity to the cytotoxic action of IAPP fibrils in two insulin-producing cell lines, HIT-T15 and RINm5F cells. *Biochem. Biophys. Res. Commun.* **251**, 888-893.

Janciauskiene, S. and Ahrén, B. (2000). Fibrillar islet amyloid polypeptide differentially affects oxidative mechanisms and lipoprotein uptake in correlation with cytotoxicity in two insulin-producing cell lines. *Biochem. Biophys. Res. Commun*. **267**, 619-625.

Kagan, B. L., Azimov, R. and Azimova, R. (2004). Amyloid peptide channels. *J. Membr. Biol.* **202**, 1-10.

Kanski, J., Varadarajan, S., Aksenova, M. and Butterfield, A. D. (2002). Role of glycine-33 and methionine-35 in Alzheimer's amyloid beta-peptide 1-42-associated oxidative stress and neurotoxicity. *Biochim. Biophys. Acta* **1586**, 190-198.

Kawahara, M., Kuroda, Y., Arispe, N. and Rojas, E. (2000). Alzheimer's β-amyloid, human islet amylin, and prion protein fragment evoke intracellular free calcium elevations by a common mechanism in a hypothalamic GnRH neuronal cell line *J. Biol. Chem.* **275**, 14077-14083.

Kayed, R., Head, E., Thompson, J. L., McIntire, T. M., Milton, S. C., Cotman, C. W. and Glabe, C. G. (2003). Common structure of soluble amyloid oligomers implies common mechanism of pathogenesis. *Science* **300**, 486-489.

Kourie, J. I. and Henry, C. L. (2002). Ion channel formation and membrane-linked pathologies of misfolded hydrophobic proteins: the role of dangerous unchaperoned molecules. *Clin. Exp. Pharmacol. Physiol*. **29**, 741-753.

Kranenburg, O., Kroon-Batenburg, L. M. J., Reijerkerk, A., Wu, Y.-P., Voest, E. E. and Gebbink, M. F. B. G. (2003). Recombinant endostatin forms amyloid fibrils that bind and are cytotoxic to murine neuroblastoma cells *in vitro*. *FEBS Lett*. **539**, 149-155.

Kruman, I. I., Pedersen, W. A., Springer, J. E. and Mattson, M. P. (1999). ALS-linked Cu/Zn-SOD mutation increases vulnerability of motor neurons to excitotoxicity by a mechanism involving increased oxidative stress and perturbed calcium homeostasis. *Exp. Neurol.* **160**, 28-39.

Lane, N. J., Balbo, A., Fukuyama, R., Rapoport, S. I. and Galdzick, Z. (1998). The ultrastructural effects of beta-amyloid peptide on cultured PC12 cells: changes in cytoplasmic and intramembranous features. *J. Neurocytol.* **27**, 707-718.

Lange, Y. and Ramos, B. V. (1983). Analysis of the distribution of cholesterol in the intact cell. *J. Biol. Chem.* **258**, 15130-15134.

Ledesma, M. D. and Dotti, C. G. (2005). The conflicting role of brain cholesterol in Alzheimer's disease: lessons from the brain plasminogen system. *Biochem. Soc. Symp*. **72**, 129-138.

Lee, E. N., Lee, S. Y., Lee, D., Kim, J. and Paik, S. R. (2003). Lipid interaction of alpha-synuclein during the metal-catalyzed oxidation in the presence of Cu2+ and H_2O_2. *J. Neurochem*. **84**, 1128-1142.

Lundin, A. (2000). Use of firefly luciferase in ATP-related assays of biomass, enzymes, and metabolites. *Methods Enzymol.* **305**, 346-370.

Mattson, M. P. (1999). Impairment of membrane transport and signal transduction systems by amyloidogenic proteins. *Methods Enzymol.* **309**, 733-768.

Mattson, M. P. and Liu, D. (2002). Energetics and oxidative stress in synaptic plasticity and neurodegenerative disorders. *Neuromol. Med.* **2**, 215-231.

Mazziotti, M. and Perlmutter, D. H. (1998). Resistance to the apoptotic effect of aggregated amyloid-β peptide in several different cell types including neuronal- and hepatoma-derived cell lines. *Biochem. J.* **332**, 517-524.

Michalik, A. and Van Broeckhoven, C. (2003). Pathogenesis of polyglutamine disorders: aggregation revisited. *Hum. Mol. Genet.* **12**, R173-R186.

Milhavet, O. and Lehmann, S. (2002). Oxidative stress and the prion protein in transmissible spongiform encephalopathies. *Brain Res. Rev.* **38**, 328-339.

Moore, N. F., Patzer, E. J., Barenholz, Y. and Wagner, R. R. (1977). Effect of phospholipase C and cholesterol oxidase on membrane integrity, microviscosity, and infectivity of vesicular stomatitis virus. *Biochemistry* **16**, 4708-4715.

Morishima, Y., Gotoh, Y., Zieg, J., Barrett, T., Takano, H., Flavell, R., Davis, R. J., Shirasaki, Y. and Greenberg, M. E. (2001). Beta-amyloid induces neuronal apoptosis *via* a mechanism that involves the c-Jun N-terminal kinase pathway and the induction of Fas ligand. *J. Neurosci*. **21**, 7551-7560.

Mruthinti, S., Hill, W. D., Swamy-Mruthinti, S. and Buccafusco, J. J. (2003). Relationship between the induction of RAGE cell-surface antigen and the expression of amyloid binding sites. *J. Mol. Neurosci*. **20**, 223-232.

Orrenius, S., Zhovotovsky, B. and Nicotera, P. (2003). Regulation of cell death: the calcium–apoptosis link. *Nat. Rev*. **4**, 552-565.

Pinton, P., Ferrari, D., Magalhaes, P., Schulze-Osthoff, D., Di Virgilio, F., Pozzan, T. and Rizzuto, R. (2000). Reduced loading of intracellular Ca^{2+} storse and downregulation of capacitative Ca^{2+} influx in Bcl-2 overexpressing cells. *J. Cell Biol.* **148**, 857-862.

Relini, A., Torrassa, S., Rolandi, R., Ghiozzi, A., Rosano, C., Canale, C., Bolognesi, M., Plakoutsi, G., Bucciantini, M., Chiti, F. et al. (2004). Monitoring the process of HypF fibrillization and liposome permeabilization by protofibrils. *J. Mol. Biol*. **338**, 943-957.

Ross, C. A. (2002). Polyglutamine pathogenesis: emergence of unifying mechanisms for Huntington's disease and related disorders. *Neuron* **35**, 819-822.

Saborido, A., Delgado, J. and Megias, A. (1999). Measurement of

sarcoplasmic reticulum Ca^{2+}-ATPase and E-type Mg^{2+}-ATPase activity in rat heart homogenates. *Anal. Biochem.* **268**, 79-88.

Sakahira, H., Brauer, P., Hayer-Hartl, M. K. and Hartl, U. (2002). Molecular chaperones as modulators of polyglutamine protein aggregation and toxicity. *Proc. Natl. Acad. Sci. USA* **99**, 16412-16418.

Sherman, M. Y. and Selkoe, A. L. (2001). Cellular defenses against unfolded proteins: A cell biologist thinks about neurodegenerative diseases. *Neuron* **29**, 15-32.

Sirangelo, I., Malmo, C., Iannuzzi, C., Mezzogiorno, A., Bianco, M. R., Papa, M. and Irace, G. (2004). Fibrillogenesis and cytotoxic activity of the amyloid-forming apomyoglobin mutant W7FW14F. *J. Biol. Chem.* **279**, 13183-13189.

Soriano, F. X., Galbete, J. L. and Forloni, G. (2003). Effect of β-amyloid on endothelial cells: lack of direct toxicity, enhancement of MTT-induced cell death and intracellular accumulation. *Neurochem. Int.* **43**, 251-261.

Sousa, M. M., Cardoso, I., Fernandes, R., Guimaraes, A. and Saraiva, M. J. (2001). Deposition of transthyretin in early stages of familial amyloidotic polyneuropathy. *Am. J. Pathol.* **159**, 1993-2000.

Squier, T. C. (2001). Oxidative stress and protein aggregation during biological aging. *Exp. Gerontol.* **36**, 1539-1550.

Stefani, M. and Dobson, C. M. (2003). Protein aggregation and aggregate toxicity: new insights into protein folding, misfolding diseases and biological evolution. *J. Mol. Med.* **81**, 678-699.

Sung, Y. J., Cheng, C. I., Chen, C. S., Huang, H. B., Huang, F. L., Wu, P. C., Shiao, M. S. and Tsay, H. J. (2003). Distinct mechanisms account for beta-amyloid toxicity in PC12 and differentiated PC12 neuronal cells. *J. Biomed. Sci.* **10**, 379-388.

Svanborg, C., Agerstam, H., Aronson, A., Bjerkvig, R., Duringer, C., Fischer, W., Gustafsson, L., Hallgren, O., Leijonhuvud, I., Linse, S. et al. (2003). HAMLET kills tumor cells by an apoptosis-like mechanism – cellular, molecular, and therapeutic aspects. *Adv. Cancer Res.* **88**, 1-29.

Tantral, L., Malathi, K., Kohyama, S., Silane, M., Berenstein, A. and Jayaraman, T. (2004). Intracellular calcium release is required for caspase-3 and -9 activation. *Cell Biochem. Funct.* **22**, 35-40.

Velez-Pardo, C., Arroyave, S. T., Lopera, F., Castano, A. D. and Jimenez Del Rio, M. (2001). Ultrastructure evidence of necrotic neural cell death in familial Alzheimer's disease brains bearing presenilin-1 E280A mutation. *J. Alzheimers Dis.* **3**, 409-415.

Walsh, D. M., Klyubin, I., Fadeeva, J. V., Cullen, W. K., Anwyl, R., Wolfe, M. S., Rowan, M. J. and Selkoe, D. J. (2002). Naturally secreted oligomers of amyloid β protein potently inhibit hippocampal long-term potentiation *in vivo*. *Nature* **416**, 535-539.

Wells, K., Farooqui, A. A., Liss, L. and Horrocks, L. A. (1995). Neural membrane phospholipids in Alzheimer disease. *Neurochem Res.* **20**, 1329-1333.

Yip, C. M. and McLaurin, J. (2001). Amyloid-β peptide assembly: a critical step in fibrillogenesis and membrane disruption. *Biophys. J.* **80**, 1359-1371.

Zhang, Y., McLaughlin, R., Goodyer, C. and LeBlanc, A. (2002). Selective cytotoxicity of intracellular amyloid b peptide$_{1-42}$ through p53 and Bax in cuyltured primary human neurons. *J. Cell Biol.* **156**, 519-529.

Zhu, M., Souillac, P. O., Ionescu-Zanetti, C., Carter, S. A. and Fink, A. L. (2002). Surface-catalyzed amyloid fibril formation. *J. Biol. Chem.* **277**, 50914-50922.